Y_2O_3:SiO_2 binary oxide: synthesis and structural characterization

RACHNA, P. AGHAMKAR
Department of Physics, Materials Science Lab., Ch. Devi Lal University, Sirsa-125055, Haryana, India

Y $(NO_3)_3.4H_2O$ and TEOS were used as precursors and powdered form of Y_2O_3:SiO_2 binary oxide was prepared by sol gel process. The powdered sample was annealed at 750^{o}C temperature and characterized by X-ray diffraction, Fourier transforms infrared spectroscopy and transmission electron microscopy. The sample analyzed by FTIR and TEM confirmed the grain size dependency on sintering temperature. Cubic structure of yttrium oxide nanocrystallite with average size ~ 21 nm was obtained at 750 ^{o}C (6h) along with crystalline silica.

(Received February 18, 2013; accepted September 18, 2013)

Keywords: Binary Oxide, Yttrium Oxide, Silica Matrix

1. Introduction

There is a growing interest in nanostructured inorganic materials because they often exhibit properties distinct from those of the bulk, which can prove their usefulness in various applications. Yttrium oxide is one of the seventeen rare earth oxide that finds use in a variety of applications including optics, display devices, X-ray imaging, core-shell materials and also as additive for liquid phase sintering of ceramics [1-3]. Yttrium oxide nanoparticles have received much attention due to their various properties and they are significantly used in fundamental and application oriented fields [4-6]. Nanocrystalline Y_2O_3 has been widely investigated due to its interesting applications in the field of phosphors for lighting and for cathode ray tube [7-8]. Oxide nanoparticles embedded in a polymer matrix also produce nanocomposites which are useful for optical and electronic applications [9]. From this point of view, amorphous silica represents the ideal candidate for rare earth metals both because of its transparency and its stabilizing effect on the nanoparticles, protecting them aggregation. Some authors have represented the use of silica for coating [10] or as a dispersing medium [11] by impregnation for doped yttrium nanoparticals. Nanocrystalline Y_2O_3 has already been synthesized by various methods such as hydrothermal [12], combustion synthesis [13] and co-precipitation [14] techniques. In the present article, sol gel technique is being used for the preparation of Y_2O_3 nanocrystallites in a silica matrix. The sol gel processes combine the advantage of lower temperature and possibility of making of finely dispersed powders, films, fibers and coating [15]. The development of a new rare-earth oxide-silica binary systems and their characterization are important not only for technological reasons but also for obtaining a better understanding. Literature survey [16, 17] reveals that formation of rare-earth oxides/silicates inside or at the surface of amorphous SiO_2 matrix depends on the synthesis method, rare-earth oxide and silica molar ratio and thermal/pressure treatment.

Some researchers [18] synthesized Y_2O_3:SiO_2 binary oxide by sol gel method but they observed that yttrium nanoparticles do not grow with thermal treatment even at 900^{0}C and 1300^{0}C. So we limit the annealing temperature at 750^{0}C in this work, because the literature showed that if annealed at 1000^{0}C or higher temperature a reaction between Y_2O_3 and SiO_2 occur, resulting in the formation of impurity like Y_2SiO_5 [19]. In this paper, we investigated the structural properties of Y_2O_3-SiO_2 binary oxide obtained by sol gel method and examine the influence of heat treatment on nanoparticles through XRD, FTIR and further confirmed by TEM study.

2. Experimental

2.1 Sample preparation

Yttria- silica binary oxide was prepared by the sol gel technique. The high purity reagents: Tetraethoxysilane (Aldrich 99.999), ethanol (Merck99.9%) and double distilled water were mixed in the presence of hydrochloric acid as catalyst. For preparation of the sample the molar ratio of starting solution was taken as 2.30: 0.72: 0.30: 0.027 for H_2O:C_2H_5OH: HCl: TEOS and 2.2 wt% yttrium nitrate tetra hydrate with concentrated HNO_3 was introduced in the pre-hydrolyzed solution under heating. The solution was kept at room temperature for three weeks where aging occurred, in which networking of bonds take place. The aging process allowed further shrinkage and stiffening of the gel. The sample was further dried at 100^{o}C for 24h and grinded by pestle and mortar to obtain powdered form of the sample. The powder sample was calcined at 750^{0}C for six hours in a high temperature programmable furnace as:

$$[R_T \xrightarrow{5C/min} 250^0C\ (3h) \xrightarrow{4C/min} 500^0C\ (3h) \xrightarrow{2C/min} 750^0C\ (6h)]$$

2.2 Characterization

The as-prepared and annealed samples were characterized by an X'pert Pro X-Ray Differectometer with $Cuk_{\alpha 1}$ radiation in the range of 5^0-80^0 in steps of 0.017^0(40mA, 45KV) for the determination of crystalline structure of binary oxide. Infrared spectra of both the samples were collected from Perkin Elmer Spectrum 400 spectrophotometer in 4000-400cm^{-1} range. FTIR spectrometer was used for functional group analysis. The morphological investigations of the annealed samples were performed by Hitachi-4500 transmission electron microscope at an accelerating voltage of 80 V.

3. Results and discussion

3. 1. XRD Analysis

Fig.1 illustrates the X-ray diffraction (XRD) patterns of as-prepared and calcined sample of Y_2O_3:SiO_2 binary oxide prepared by the sol gel process. The differactogram of as-prepared sample shows amorphous nature of SiO_2 silica host with a small characteristic peak of cubic Y_2O_3. When the as-prepared sample was calcined at 750^0C, crystalline phases of both Y_2O_3 and SiO_2 were obtained in the differactogram. The XRD pattern of calcined sample shows characteristic peak of pure cubic Y_2O_3 crystallite at 2θ~29.25° along with some weak peaks at 2θ ~ 20.62°, 33.85°, 48.58 °,57.77 ° in accordance to JCPDS card no. 41-1105. Check cell program was used to find Miller indices of respective peaks, which are found to be (211), (222), (400), (440), and (622) and further confirmed the pure cubic structure of Y_2O_3 crystallite having lattice constant 'a' = 10.57A°, space group Ia3(T_h^7) with C-M_2O_3 type structure [20].

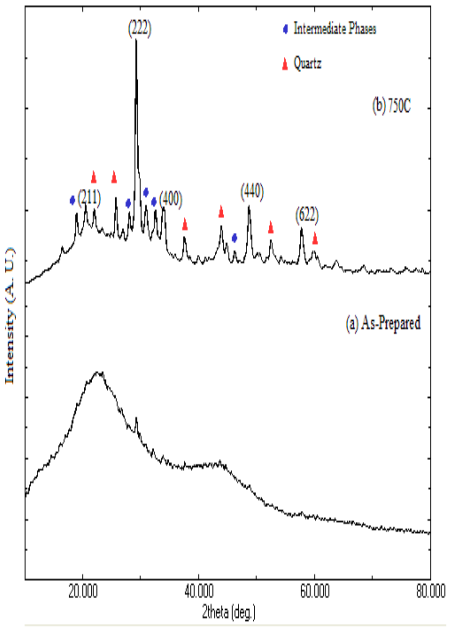

Fig.1. XRD pattern of as-prepared (a) and annealed sample (b) of Y_2O_3:SiO_2 composites.

Quartz structure of SiO_2 is identified by the diffraction peaks at 2θ ~ 20.48°, 25.74°, 37.58°, 48.76°, 52.48° (in accordance to JCPDS card no. 46-1045). Some additional peaks also appeared in the differactogram at 2θ ~ 18.96°, 28.06°, 30.94°, 32.08°, 45.67° which could be intermediate phases of yttrium oxide and silica. The crystallite size can be estimated from the well known Scherrer formula: $D_{hkl}=K\lambda/(\beta\cos\theta)$, where λ is the X-ray wavelength, θ is the diffraction angle, K is Scherrer constant (0.89), and D_{hkl} means the size along (hkl) plane. Here we have taken (222) plane to calculate average crystallite sizes of Y_2O_3:SiO_2 binary oxide and found to be ~ 21 nm.

3.1.1 Strain Analysis by W-H Plot

The XRD profile show broadening which may be due to lattice strain [21]. Due to the small crystallite size and strain present in the materials, the XRD peak broadening can be distinguished from Williamson–Hall (W–H) plot.

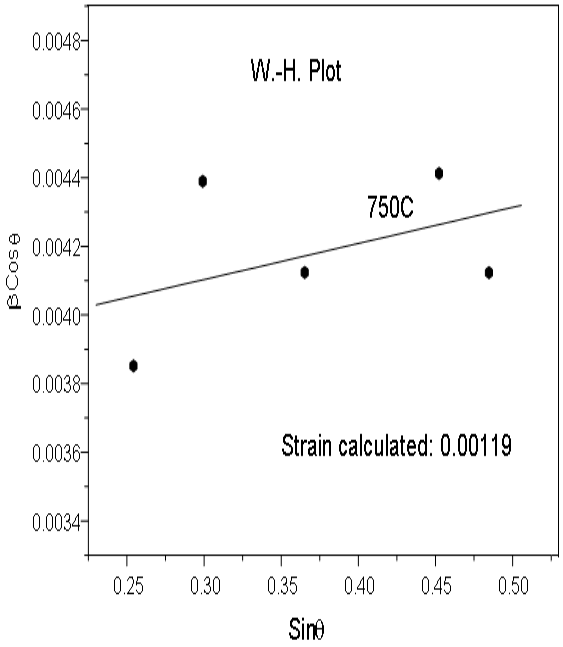

Fig.2. W-H plot for the sample annealed at 750°C.

It is well known that the crystallite size and strain contributions to line broadening are independent of each other. Here, the crystallite size was estimated from W–H plot only for annealed (750^0C) sample because of its well crystalline nature [22]. Due to the small crystallite size and strain present in the materials, the XRD peak broadening as well as the crystallite size can be distinguished from Williamson–Hall plot. The W–H equation is:

$\beta_{hkl}\cos\theta_{hkl} = K\lambda/d + 2\varepsilon\sin\theta_{hkl}$, where β_{hkl} is the full width at half maximum, ε is the strain and d is a average crystallite size measured in a direction perpendicular to the surface of the specimen. The graph was plotted between $\sin\theta_{hkl}$ and $\beta_{hkl}\cos\theta_{hkl}$ as shown in fig. 2. The value of the strain was estimated from slope of the line and the crystallite size from the intersection with the vertical axis.

The estimated crystallite size of the binary oxide from this method was in agreement with the Debye-Scherrer's equation and TEM morphological results. It was observed that the strain value was found very small ~ 0.00119 and hence the strain has negligible effect in XRD broadening. The above result suggests that the Y_2O_3:SiO_2 binary oxide synthesized by sol-gel technique thermally treated at 750^0C produces Y_2O_3:SiO_2 nanocomposite with increased crystallite size ~ 21 nm and distinct grain boundaries.

3.2 FTIR Analysis

The FTIR spectra of as prepared and annealed sample of Y_2O_3:SiO_2 binary oxides are shown in Fig. 3 within the spectral range 4000-400 cm^{-1}. These spectra provide valuable information about the phase composition as well as bonding in the sintered composites. Table 1 shows the sources and absorption bands of the FTIR spectra. The FTIR spectra of as prepared and annealed samples have three major absorption regions of Y_2O_3, SiO_2 and H_2O. In the first region, the peak at 565.91cm^{-1} is assigned for the stretching frequency of Y-O bond which originates from Y_2O_3 molecule. This lower wave number side of the as prepared FTIR spectrum shows that the Y-O absorption band become broader compared to the annealed sample. Characteristics peak of Y-O bond is well grown with thermal treatment and can be seen clearly at 560.91 cm^{-1} in FTIR spectrum (b). It is understood that the decrease in the particle size enhances the surface effects which in turn enlarge the absorption. Thus, the Y-O absorption band is widened in as-prepared sample [23].

Table1.FTIR peak positions and corresponding functional groups of Y_2O_3:SiO_2 binary oxide.

Absorption frequency (cm^{-1})	Assignment
562 cm^{-1}	Characteristic vibrational band of Y-O bond
562-803 cm^{-1}	-CH_2 streching bond
803 cm^{-1}	Si- O-Si symmetric stretching
970 cm^{-1}	Silanol group Si-OH
1087 cm^{-1}	Si- O-Si symmetric stretching in cyclic structure(asymmetric stretching)
2361.71, 1315-1360 and 1483cm^{-1}	Organic residues specially C-O, C=O in ethyl group and nitro group
1625-1650 cm^{-1}	Bending modes of H-O-H adsorbed at silica surface.
3450 – 3400 cm^{-1}	O-H vibrations of residual adsorbed water, Si-OH stretching vibrations

In the second region, the band around 468.05 cm^{-1} is due to the Si-O-Si and O-Si-O bending modes while 803.18 cm^{-1} and 1101.72 cm^{-1} correspond to the Si-O-Si symmetric and antisymmetric stretching vibrations, respectively [23, 24, 25]. The band at 970.27 cm^{-1} is due to stretching of silanol (Si-OH) group which however, gradually weakens and disappears which is an indication of phase transformation of yttrium nitrate hydrate and silica hydrate into crystalline Y_2O_3 and SiO_2 with thermal treatment. This reveals that the network structure of short-range order tetrahedral SiO_4 was destroyed and became more disordered. This behavior is typical of the silica condensation process with heat treatment.

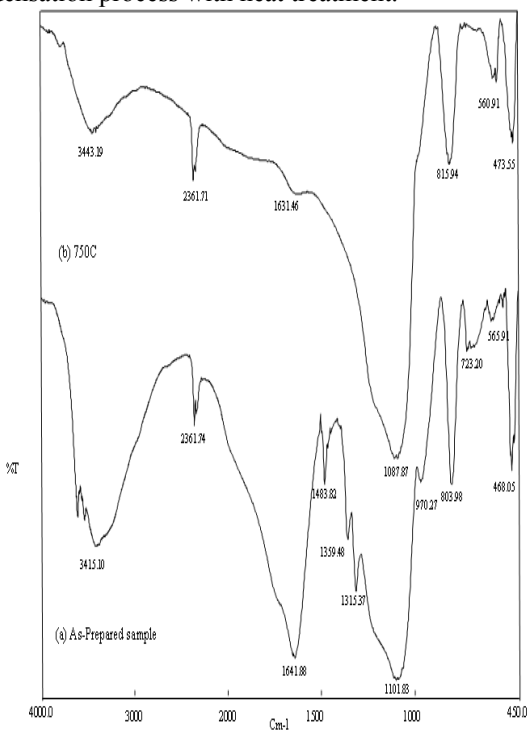

Fig.3. FTIR spectra of Y_2O_3:SiO_2 composite (a) as-prepared and (b) annealed at 750^oC.

In the third region, the as-prepared sample exhibits a broad absorption band in the region 3400-3450 cm^{-1} assigned to O-H stretching vibration and at 1641.88 cm^{-1} due to the molecular H-O-H bending modes [25]. This indicates that there exist a variety of hydroxyl groups such as isolated -OH groups, pairs of hydrogen bonded Si-O and physically adsorbed water molecules in the silica matrix. H-OH band overlaps with the surface hydroxyl group vibration and results in the broadening of band as the temperature increases. Moreover, the water signals are visible in the IR spectrum even after the thermal treatment up at 3443 and 1631 cm^{-1}. It is likely that the presence of water is partially due to the hydrophilicity of the samples or impure KBr. However, these signals attenuate but do not disappear after heating the samples at 100^0C (drying temperature) during the spectra recording which suggests that some water molecules remain inside the pores of material. The absorption peak centered at 1483.82 cm^{-1} disappeared with thermal treatment indicating the absence of nitrate form of precursors and well in agreement with

XRD data. Similarly organic residues like C=O, C-O are absent in IR spectrum at 750^0C.

3. 3. TEM Analysis

A transmission electron microscopic study of as-prepared and annealed samples has been shown in the figures 4(a-c). Networking of Si-O-Si bond can be seen easily in silica matrix given in the Fig. 4 (a). The TEM images in Fig.4 (b) confirm the narrow size distribution and grain growth process in the sintered sample at 750^0C temperature. In this condition shape of the particle is nearly spherical with well defined grain boundaries. The grain growth indicated the diffusivity of grain boundary of obtained spherical nanoparticles. Moreover, thermal treatment of the sample at comparatively high temperature (750 ^{o}C) provides much improved dispersion of Y_2O_3 in a silica matrix. The selected area electron diffraction pattern of Y_2O_3:SiO_2 composite in Fig. 4(c) supports our XRD results. The above result infer that the morphology of crystalline Y_2O_3:SiO_2 binary oxide obtained by sol gel method can be controlled by selecting correctly both the thermal treatment and used precursors.

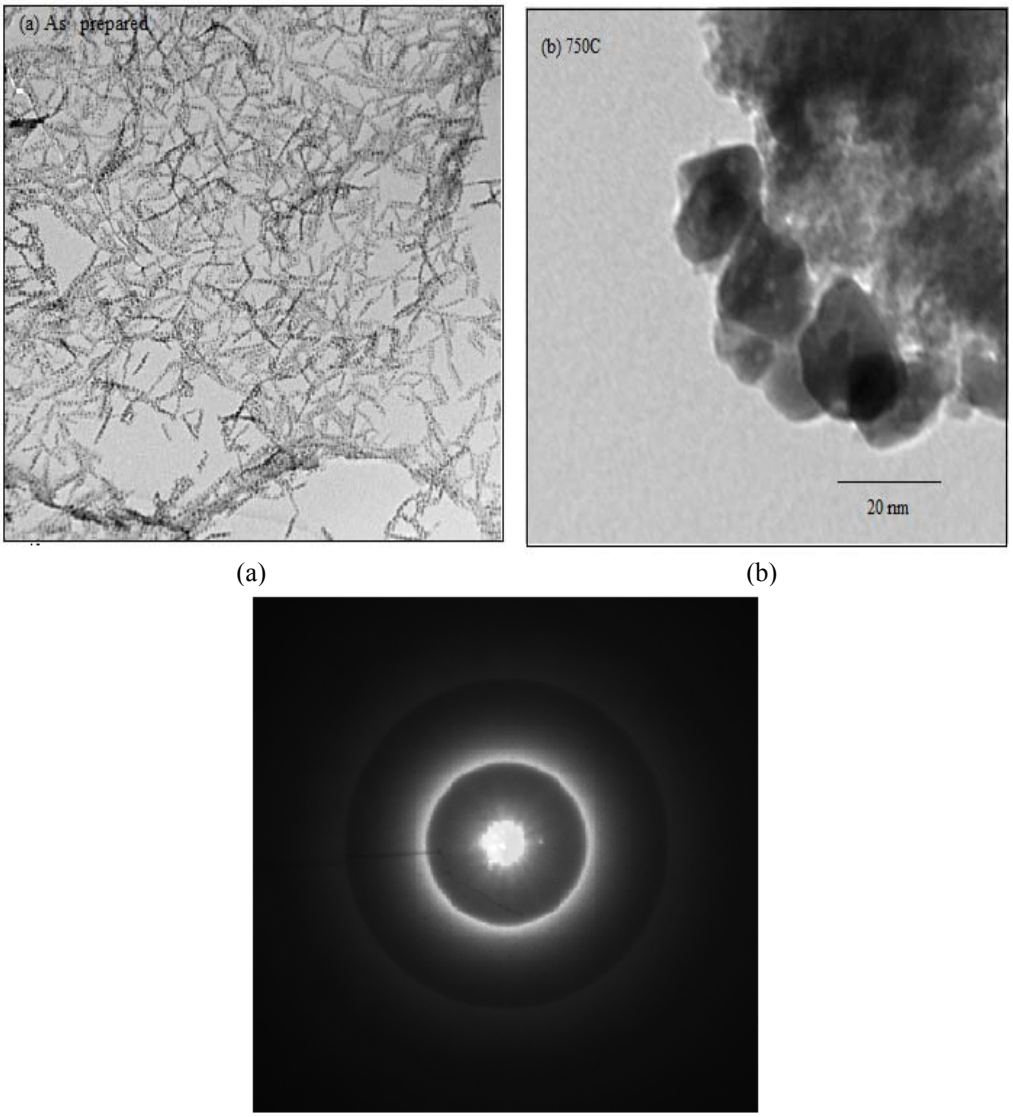

Fig.4. Transmission electron micrograph of as-prepared (a) and annealed Y_2O_3:SiO_2 composites (b) along with selected area electron diffraction pattern(c).

4. Conclusion

Using sol gel method Y_2O_3:SiO_2 binary oxide was successfully obtained upon thermal treatment in air. The XRD analysis proved that cubic structure of Y_2O_3 was well grown with quartz structure of silica. The average particle size of Y_2O_3 nanocrystallite was obtained nearly 21 nm at 750^oC calculated by Debye-Secherrer formula and W-H plot. Different functional groups have been investigated by FTIR spectra and it shows that the absorption bands broadened as the particle size decreases. Yttrium- oxygen characteristic band was appeared at 560.91 cm^{-1}.

References

[1] L. Kepinski, M. Wolcyrz, Mater. Chem. Phys. **81**, 396 (2003).

[2] K. Ariga, J.P. Hill, M.V. Lee, A. Vinu, R. Charvet, S. Acharya, Sci. Technol. Adv. Mater. **9**, 014109 (2008).

[3] J.S. Kim, M.-C. Chu, D.-S. Bae, J. Korean Cer. Soc. **45**, 512 (2008).

[4] Y. L. Kopylov, V. B. Kravchenko, A. A. Komarov, Z. M. Lebedeva, V. V. Shemet, Opt. Mater. **29**, 1236 (2007).

[5] G. Yao, L.B. Su, J. Xu, X.D. Xu, L.H. Zheng, Y. Cheng, J. Cryst. Growth, **310**, 404 (2008).

[6] R. Chaim, A. Shpayer, C. Estournes, Journal of the European Ceramic Society, **29**, 91-98 (2009).

[7] K. Takaichi, H. Yagi, J. Lu, J. Bission, A. Shirakawa, Ucda, T. Yanagitani, A.A. Kaminshii, Appl. Phys. Lett. **84**, 317 (2004).

[8] A. H. Kitai, Thin Solid Films **445**, 367 (2003).

[9] P. Aghamkar, S. Duhan, M. Singh, N. Kishore, P. K. Sen, Journal of Sol-Gel Science and Technology, **46**, 17 (2008).

[10] R. Schmechel, M. Kenedy, H. Von Seggem, H. Winkler,M. Kolbe, R. A. Fischer, Li Xaomao, A. Benker, M. Winterer,J. Appl. Phys., **89**, 1679 (2001).

[11] Q. Li, L. Gao D. Yan, Chem. Mater., **11**, 533 (1999).

[12] H. Tomaszewski, H. Weglarz, R.D. Gryse, J. Eur. Ceram. Soc. **17**, 403 (1997).

[13] T. Ye, Z. Guiwen, Z. Weiping, X. Shangda, Mater. Res. Bull. **32**, 501 (1997).

[14] R. Srinivasan, R. Yogamalar, A. Vinu, K. Ariga, A.C. Bose, J. Nanosci. Nanotechnol. **9**, 6747 (2009).

[15] L.L. Hench, J.K. West, Chem. Rev. **90**, 33 (1990).

[16] M. Zawadzki, L. Kepinski, J. Alloys Comp. **380**, 255 (2004).

[17] L. Kepinski, M. Wolcyrz, M. Drozd, Mater. Chem. Phys. **96**, 353 (2006).

[18] C. Cannas, M. Casu, A. Lai, A. Musinu, G. Piccaluga, Phys. Chem., Chem. Phys. **4**, 2286(2002).

[19] H.Wang, M. Yu, C.K. Lin, J. Lin, J. Colloid Interf. Sci. **300**, 176(2006).

[20] R. G. Haire, L. Eyring, Comparisons of the Binary Oxides, Handbook on the Physics and Chemistry of Rare Earths, North- Holland, Amsterdam, (1994).

[21] R. Ramamoorthy, S. Ramasamy, D. Sundaraman, J. Mater. Res. **14**, 90 (1999).

[22] S.T. Tan, B.J. Chen, X.W. Sun, W.J. Fan, H.S. Kwok, X.H. Zhang, S.J. Chua, J. Appl. Phys. **98**, 013505 (2005).

[23] M. Nakamura, Y. Mochizuki, K. Usami, Y. Itoh, T. Nozaki, Solid State Commun. **50**, 1079 (1984).

[24] A. Milutinovic, Z. Dohcevic-Mitrovic, D. Nesheva, M. Scepanovic, M. Grujic- Brojcin, Z.V. Popovic, Mater. Sci. Forum **555**, 309 (2007).

[25] S.Duhan, P.Aghamkar and M. Singh Research Lett. Phys. **2008**, Article ID 237023, doi:10.1155/2008/237023.(2008).

*Corresponding author: rachnaahlawat2003@yahoo.com